ELSEVIER

Journal of Molecular Catalysis A: Chemical 96 (1995) 35–48

JOURNAL OF MOLECULAR CATALYSIS A: CHEMICAL

Catalytic and structural properties of ruthenium bimetallic catalysts: kinetics of 2,2,3,3-tetramethylbutane hydrogenolysis

Bernard Coq *, Eleanor Crabb, François Figuéras

Laboratoire de Chimie Organique Physique et Cinétique Chimique Appliquées, 8, rue de l'Ecole Normale, 34053 Montpellier, France

Received 13 April 1994; accepted 7 October 1994

Abstract

The kinetics of 2,2,3,3-tetramethylbutane (TeMB) hydrogenolysis has been investigated over alumina-supported mono- and bimetallic ruthenium catalysts. The bimetallic catalysts were prepared from the monometallic ones by controlled surface modification with Sn, Pb and Ge organometallics. As reported earlier, large Ru particles (> 3 nm) favour the cleavage between the two quaternary carbon atoms leading to isobutane ($\alpha\delta$ process); moreover, deep hydrogenolysis of the adsorbed alkyl fragments occurs before desorption. At the opposite, on small Ru particles (≈ 1 nm) demethylation to 2,2,3-trimethylbutane is the main reaction ($\alpha\gamma$ process) and deep hydrogenolysis is suppressed. The addition of Sn or Pb onto small Ru particles has only a small effect on the reaction rate but shifts the selectivity pattern towards that of large Ru particles, while the selectivity remains unchanged upon Ge addition. The addition of either Sn or Ge to large Ru particles decreases the rate by two orders of magnitude. With respect to the rate, hydrogen has a stronger inhibiting effect on the sample of lower dispersion. Both rates for $\alpha\gamma$ and $\alpha\delta$ processes go through a maximum as a function of hydrogen pressure, the maximun for the $\alpha\delta$ process being shifted to higher H_2 pressures. Assuming (i) Langmuir adsorption isotherms, (ii) multisite competitive adsorption between hydrogen and TeMB, (iii) hydrogenation of the dehydrogenated adsorbed alkane (most abundant surface intermediate, MASI) by a surface hydrogen atom as the rate determining step, a rate law was proposed for both $\alpha\gamma$ and $\alpha\delta$ processes. The kinetic analysis suggests that highly dehydrogenated intermediates ($\alpha\delta$ process, -5H) are formed on large Ru particles. These species need a large ensemble of Ru atoms to be formed. At variance, on small Ru particles hydrogenolysis could proceed through less dehydrogenated adsorbed species: metallacyclobutane for the $\alpha\gamma$ process (-2H) and metallacyclopentane for the $\alpha\delta$ process (-3H), the formation of the latter being inhibited at high H_2 pressure. These metallacycles can be formed on small ensembles of Ru atoms. The addition of Sn or Ge to small Ru particles does not change very much the positions of the rate maxima for $\alpha\gamma$ and $\alpha\delta$ processes, or the hydrogen dependence of the rate. It emerges that the main effect of Sn and Ge addition is to decrease the number of sites active for $\alpha\gamma$ and $\alpha\delta$ processes respectively, the former being the sites of low coordination, the latter the sites of high coordination.

Keywords: Bimetallic catalysts; Hydrogenolysis; Kinetics; Ruthenium; Supported catalysts; Tetramethylbutane

1. Introduction

The hydrogenolysis of 2,2,3,3-tetramethybutane (TeMB) over supported metals is extremely sensitive to the coordination of surface metal atoms for Rh [1], Pt [2] and Ru [3] catalysts. On high coordination number atoms, dense planes and large particles, the preferred reaction is C-C splitting between the two quaternary carbon atoms (C_Q) leading to isobutane as the primary product ($\alpha\delta$ process). On low coordination number

* Corresponding author. Fax: (+33)67144395

SSDI 1381-1169(94)00028-X

atoms, corners and edges of small particles, the demethylation of TeMB to 2,2,3-trimethylbutane (TriMB) and CH_4 ($\alpha\gamma$ process) becomes important, or even selective as in the case of Rh/Al_2O_3 [1]. The $\alpha\gamma$ and $\alpha\delta$ processes could occur through metallacyclobutane and metallacyclopentane respectively, bonded to one or more metal atoms. The occurrence of these two kinds of surface complexes has been confirmed by TeMB/D_2 exchange on Rh and Ru [4,5]. Moreover, TeMB/D_2 exchange showed that small Rh particles exhibit a greater ability to form $\alpha\gamma$ complexes than larger ones [6]. It turns out that selectivity in TeMB hydrogenolysis varies most for metal particles smaller than 2 nm. At 101 kPa H_2 pressure, and whatever the metal, particles larger than 2 nm give iC_4 selectively (>90%) as the primary product, whereas metal particles smaller than 1 nm yield only 50% iC_4 for Pt at 553 K [2], 45% for Ru at 473 K [3], and less than 5% for Rh at 493 K [1]. Thereby, this reaction constitutes a powerful molecular probe for identifying subtle changes in the surface topology of small metal particles. For instance, it has allowed us to determine the surface site distribution of the two elements in RuM [7], PtM [2] and RhM [1] bimetallic catalysts (where M = Sn, Pb, Ge). It was shown that a small additions of Sn or Pb favour the $\alpha\delta$ process, whereas Ge had an opposite effect. Quantum chemical calculations [1] supported the view that Sn and Pb segregate to low coordination sites, while Ge does not have such a definite preference. This concept of surface site segregation was first introduced by the pioneering work of Burton et al. [8]. Catalytic reactions, usually alkane hydrogenolysis, to probe the surface site distribution were also used for $RhCu/SiO_2$ [9] and $RuCu/SiO_2$ [10] catalysts. However, activity and selectivity in alkane hydrogenolysis is highly dependent on the H_2 pressure as shown, for instance, for n-butane hydrogenolysis on Ru/Al_2O_3 [11]. Thus, particle size or bimetallic effects might be obscured or exaggerated depending upon the reaction conditions used; erroneous conclusions might then be derived from such behaviours. It was therefore the aim of this work to validate the use of TeMB hydrogenolysis as a probe for Ru surfaces, by studying the kinetics of the reaction on a series of mono- and bimetallic RuM/Al_2O_3 catalysts (M = Sn, Pb, Ge). Special attention will be paid to the mechanism of the reaction, the nature of the surface complexes and of the active centres.

2. Experimental

2.1. Preparation and characterisation of the catalysts

Full details concerning the preparation and the characterisation of the catalysts were given in a previous study [12]. We shall recall here the most salient points of the preparation and the main characteristics of the samples. The monometallic parent catalysts (RuEC1 and RuEC3) were prepared by contacting ruthenium acetylacetonate ($Ru(acac)_3$, Heraeus) in toluene solution with γ-Al_2O_3 (Rhône Poulenc, $S_{BET} = 220\ m^2\ g^{-1}$). The solution was either filtered (RuEC1), or the solvent was evaporated (RuEC3). After drying under vacuum at 333 K the resulting solids were first dried under N_2 at 473 K, then reduced under different conditions. The monometallics RuEC1 and RuEC3 were used as the bases for the bimetallic formulations. The second metal was introduced as tetra-n-butyl tin (Merck, purity > 98%), tetra-ethyl lead (Alfa Products) or tetra-n-butyl germanium (Alfa Products). The bimetallic RuM/Al_2O_3 samples were prepared by contacting in situ a prereduced Ru/Al_2O_3 parent catalyst with the desired amount of tetra-alkyl-M in n-heptane solution. The controlled surface reaction [7,13,14] was carried out under an H_2 atmosphere at 353 K. The solid was dried at 333 K under N_2 and then reduced under H_2 at 623 K to obtain true bimetallic particles.

Basic characteristics of these catalysts were obtained from TPR and TPO experiments, H_2 and CO chemisorption, TEM examination, XPS and EXAFS studies [12]. Here will only be presented the values for H_2 chemisorption carried out at 373 K in a static volumetric apparatus with the single

Table 1
Main characteristics of the alumina supported Ru catalysts

Catalyst	Ru content (wt%)	2nd metal content (M = Ge, Sn, Pb)			H/Ru
		(wt%)	M/Ru (at/at)	M/Ru_s (at/at) [a]	
RuEC1	0.97	–			0.88
RuEC3	4.0	–			0.25
RuEC1Ge1	0.97	0.15	0.23	0.39	0.59
RuEC1Ge3	0.97	0.70	1.06	2.6	0.41
RuEC1Sn1	0.97	0.26	0.24	0.47	0.51
RuEC1Sn2	0.97	0.54	0.50	1.56	0.32
RuEC1Pb1	0.97	0.51	0.26	0.40	0.66
RuEC3Ge1	4.0	0.41	0.15	1.25	0.12
RuEC3Sn1	4.0	0.51	0.12	0.63	0.19

[a] Ru_s surface Ru atoms.

isotherm method (Table 1). The agreement for the Ru particle sizes, in monometallic samples, determined from H_2 chemisorption and electron microscopy, was good.

2.2. Catalytic experiments

The reaction of 2,2,3,3-tetramethylbutane (TeMB, Aldrich >99%) with hydrogen (high purity grade >99.99%) was studied by performing kinetic measurements at different hydrogen pressures in a stainless steel reactor operated at low conversion (typically less than 5%) in order to minimize readsorption of the products and to avoid heat and mass transfer limitations. The TeMB partial pressure was maintained constant at 1.3 kPa. The effluents were analysed by sampling on-line to a gas chromatograph equipped with a J and W capillary column (30 m × 0.5 mm i.d., DB1 apolar bonded phase).

An aliquot of the catalyst, typically 50 or 100 mg, was pretreated in situ by reduction in flowing hydrogen (20 cm^3 min^{-1}) up to 623 K (heating rate 1 K min^{-1}), remaining at this temperature for 3.5 h before cooling down to the initial reaction temperature (413 K). The typical range of reaction temperatures studied was 413-493 K, depending on the activity of the sample. For the initial screening experiments, the heating rate was controlled at 0.5 K min^{-1} over this range, until the top temperature was reached, remaining isothermal at this temperature for 60 min before starting the downward ramp. The hydrogen flow was reduced to 10 cm^3 min^{-1} for the reaction. As some decay of activity was observed in the initial screening (typically 30-50%), the following protocol for the catalytic test was adopted in order to stabilise the catalysts. TeMB hydrogenolysis was first carried out over the range 433-493 K at atmospheric pressure (flow 20 cm^3 min^{-1}, heating ramp 0.5 K min^{-1}) and the reaction held at 493 K for 4 h before cooling to 433 K at 0.5 K min^{-1}. The catalysts were then left overnight at this temperature in a stream of hydrogen (20 cm^3 min^{-1}). The catalyst was then tested at atmospheric pressure for the hydrogenolysis of TeMB over the same temperature range but without the isothermal portion at 493 K. This procedure was repeated at 202, 353 and 504 kPa total pressure, again at 101 kPa, to ensure that there was no great modification in the catalyst properties and then at 49.8, 24.9 and 12.5 kPa hydrogen partial pressure (101 kPa total pressure, with He as the diluent). The catalyst was heated at 433 K in a stream of hydrogen (20 cm^3 min^{-1}) overnight between each test.

An additional experiment was carried out to monitor the hydrogenolysis of TeMB over the first 30 min of the reaction course. A 100 mg sample of catalyst was reduced in hydrogen (10 cm^3 min^{-1}) at 623 K, then cooled to the reaction temperature of 445 K. After that, the TeMB was switched on. A 16-port sampling valve, with sample loops of 0.8 cm^3, was used to store in sequence the reaction products. Samples were taken every 15 s initially, with intervals increasing over time. The stored samples were then analyzed at a later time by flushing each loop with N_2 to the sampling valve (20 μl loop) of the GC apparatus.

The following parameters were evaluated:

conversion (mol%)

$$= \left(\sum_{1}^{8}(i/8)C_i\right) / \left(C_8^0 + \sum_{1}^{8}(i/8)C_i\right) \times 100$$

selectivity S_i to compound i:

$$S_i\,(\text{mol\%}) = C_i/(\sum_1^8 C_j) \times 100$$

where C_i is the mole percent in the feed of product with i carbon atoms and C_8^0 is the mole percent in the feed of TeMB.

The turnover frequency (TOF) is defined as the number of molecules of reactant transformed per unit time and per surface Ru atom.

The depth of hydrogenolysis, or number of fragments produced from one molecule of reactant before desorption, was characterised by the fragmentation factor defined, following Paal and Tetenyi [15], as:

$$\xi = \sum_1^8 C_i / \sum_1^7 (i/8) C_i$$

3. Results

First we will recall some important features of the Ru catalysts reported elsewhere [12,16]. The Ru particles in the RuEC1 sample are extremely small as shown by H_2 and CO chemisorption (H/Ru = 0.88, CO/Ru = 1.31), TEM examination (particle sizes in the range 0.8-1.5 nm) and EXAFS studies. From these experiments it was shown that the average coordination number of Ru is of 4.35 (Ru^0-Ru^0 + Ru^0-$Ru^{\delta+}$) and the Ru-Ru distances shorter (2.60 Å) than the bulk one (2.67 Å). Furthermore, this sample contains some partially oxidised Ru atoms (10-15%), even after reduction at 623 K in flowing hydrogen. On the other hand, the large Ru particles of the RuEC3 sample exhibit coordination numbers and Ru-Ru distances the same as the bulk values (CN = 12, Ru-Ru = 2.67 Å). In the bimetallic samples, prepared according to the controlled surface reaction technique, the size of the metallic particles was not modified by adding Ge, Sn or Pb, and the intimate contact between Ru and Ge was confirmed by EXAFS [16].

The transient kinetics was studied during the first seconds of TeMB conversion over the H-precovered Ru surface of RuEC1 sample. Fig. 1 shows the reaction rate and selectivities versus reaction time for the first 15 min of reaction at 445 K. The delay time between switching on TeMB and the first detection of the hydrocarbon in the effluent corresponds to 180 s. The total peak area reached its maximum value after about 300 s. It can be seen that the selectivity to CH_4, which is initially the dominant product, decreases with time until it reaches a steady value at about 45% after 240 s. The selectivity to iC_4 increases, going through a slight maximum of 28% at 190-210 s,

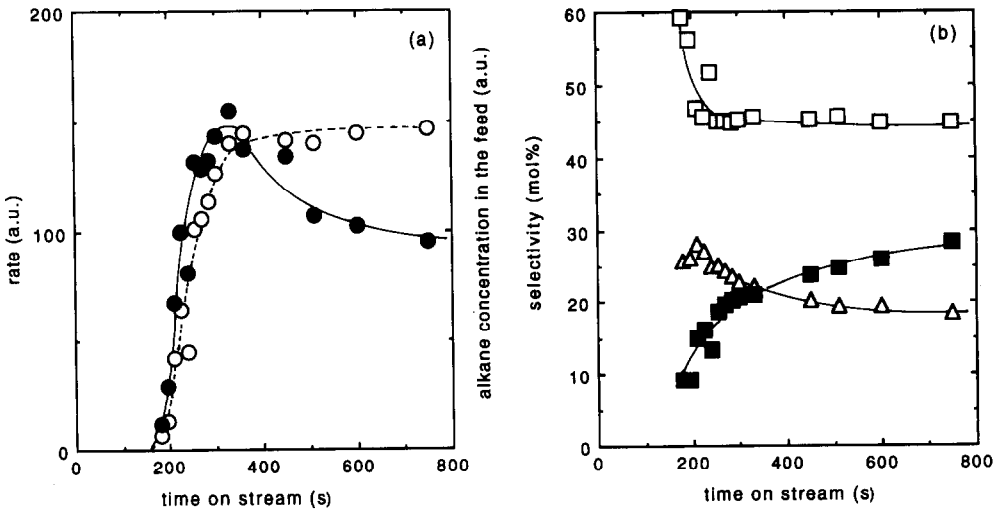

Fig. 1. Transient period of TeMB hydrogenolysis on RuEC1 catalyst at 445 K: (a) alkane concentration (GC peak area) in the feed (○), and reaction rate (●); (b) selectivity for CH_4 (□), iC_4 (■), TriMB (■). P_H = 99.7 kPa, flow rate = 0.17 ml s^{-1}.

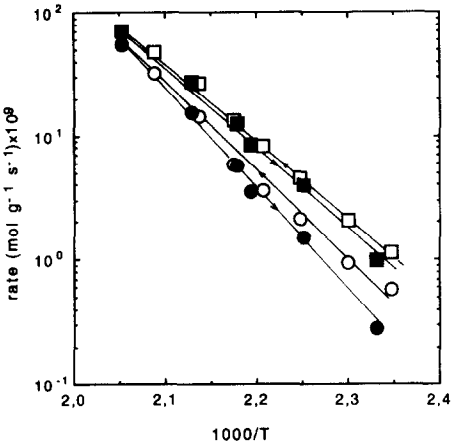

Fig. 2. Arrhenius plots for TeMB hydrogenolysis on RuEC1 catalyst; open symbols: increasing ramp; full symbols: decreasing ramp; (□,■) $\alpha\gamma$ process, (○,●) $\alpha\delta$ process. P_H = 99.7 kPa.

before decreasing to a constant value of approximately 20%, after about 420 s. The selectivity to 2,2,3-trimethylbutane (TriMB) is initially very low, at just 9%, increasing steadily with time until it reaches a value of about 29% after 900 s. Due to the parallel enhancement of the selectivity for iC_4 and TriMB during the first 100 s, it is clear that multiple fission to methane starts from iC_4^* and TriMB* adsorbed fragments. It would appear that the main changes of selectivity occur during the transient period where the TeMB concentration increases in the feed. As soon as it reaches its maximum value (at $\approx$ 300 s) the selectivity changes are smaller. After 900 s, a total of 0.2 mol of TeMB per mole of surface ruthenium atom has been converted, and the catalytic properties remain stable. It is very likely that carbon deposition decreases the multiple fragmentation of adsorbed TeMB, and favours the $\alpha\gamma$ process in comparison with the $\alpha\delta$ one.

Fig. 2 shows typical Arrhenius plots obtained for the RuEC1 sample, after the passivation period and according to the protocol described in the experimental section. Since a slight deactivation always occurs between the increasing and the decreasing ramp, the latter was used to derive the kinetic results. All the samples were tested following the same procedure.

Table 1 reports the main catalytic properties for TeMB conversion over RuM/Al_2O_3 and the parent monometallic catalysts for the initial screening experiments. The results are in full agreement with those previously reported on the effects of Ru particle size [3] and of 'alloying' ruthenium [7] on TeMB hydrogenolysis over similar catalysts. On pure Ru/Al_2O_3 catalysts (RuEC1 and RuEC3) a strong effect of particle size is observed, both on TOF and on selectivities. When the Ru dispersion is increased, the TOF and deep hydrogenolysis decrease, and the fragmentation factor ξ becomes close to a value of 2 on the RuEC1 sample; the selectivity for TeMB hydrogenolysis is shifted from splitting of the central bond ($\rightarrow 2$ iC_4) to demethylation ($\rightarrow CH_4$ + TriMB). The addition of a small amount of Sn or Pb to the well dispersed RuEC1

Table 2
Main catalytic properties of Ru catalysts for the hydrogenolysis of TeMB. P_H = 99.7 kPa; TeMB partial pressure = 1.3 kPa

Catalyst	Temp. (K)	Conv. (mol%)	TOF (s^{-1})x10^4	Selectivity (mol%)					ξ
				C_1	C_2–C_3	iC_4	C_5–C_6	TriMB	
RuEC1	459	0.95	2.2	38.7	–	29.6	1.2	30.5	2.12
RuEC1Sn1	465	0.60	2.0	29.4	–	48.5	–	22.0	2.12
RuEC1Sn2	473	0.10	0.75	42.3	–	20.0	–	37.7	2.07
RuEC1Ge1	463	1.0	3.5	40.4	0.8	28.5	4.5	25.2	2.15
RuEC1Ge3	460	0.75	0.75	43.6	–	16.0	–	40.4	2.06
RuEC1Pb1	464	1.50	4.4	31.6	1.7	40.5	3.8	22.4	2.11
RuEC3	436	8.3	16.7	32.7	11.1	50.9	5.3	2.2	2.70
"	468	56	104	85.6	19.1	9.2	2.4	0.2	4.54
RuEC3Ge1	438	1.70	0.6	12.4	2.4	80.4	–	4.9	2.14
RuEC3Sn1	433	0.30	0.7	30.0	7.8	59.2	–	3.0	2.61

Table 3
Main catalytic properties for the hydrogenolysis of TeMB at 463 K and different hydrogen partial pressures on RuEC1 catalyst. TeMB partial pressure = 1.3 kPa. Rows are presented following the sequence of experiments

Pressure (kPa)		TOF (s^{-1}) x10^4	Selectivity (mol%)					ξ
Total	P_H		C_1	C_2–C_3	iC_4	C_5–C_6	TriMB	
101	99.7	2.9	38.9	0.9	30.3	1.6	28.4	2.12
202	200.7	2.0	43.2	0.8	22.5	0.9	32.6	2.13
353	351.7	1.15	43.5	0.6	19.0	1.8	35.1	2.12
504	503.7	0.58	42.3	–	17.4	0.8	39.5	2.03
101	99.7	2.4	37.8	0.7	30.9	1.9	28.7	2.13
101	49.8	2.2	36.9	1.5	41.5	2.4	17.7	2.31
101	24.9	2.6	32.7	3.4	46.5	4.0	13.4	2.33
101	12.5	1.9	37.3	5.2	40.9	3.7	12.9	2.47

Table 4
Kinetic results for the hydrogenolysis of TeMB at different hydrogen partial pressures over RuEC1 catalyst. TeMB partial pressure = 1.3 kPa

P_H (kPa)	Route $\alpha\delta$			Route $\alpha\gamma$		
	Rate [a]	E_a (kJ mol^{-1})	ln$A$ [b]	Rate [a]	E_a (kJ mol^{-1})	ln$A$ [b]
12.5	8.88	123	22.8	7.53	124	23.0
24.9	12.1	162	33.2	9.53	137	26.6
49.8	9.12	156	31.5	9.17	152	30.3
99.7	6.12	163	32.8	14.3	139	27.5
99.7	8.20	155	31.1	16.8	128	24.9
200.7	4.03	161	31.8	12.5	132	25.6
351.7	2.03	155	29.6	7.83	141	27.4
503.7	0.85	160	30.2	4.17	144	27.6

[a] Reaction temperature: 463 K; rate in (mol s^{-1} g^{-1}) × 10^9.
[b] A in s^{-1}.

sample shifts the selectivity pattern towards that of large Ru particles with an increase in iC_4, while the selectivity remains approximately the same for a similar addition of Ge. These effects were attributed to the preferential occupancy of defect sites, edges and corners, by Sn or Pb in bimetallic particles [7], as predicted by the theory of site segregation [8]. Ge does not have such a definite preference and could be more randomly distributed. At higher Sn or Ge content, the properties of RuEC1 for TeMB hydrogenolysis are shifted towards those of smaller particles, in both cases; the classical phenomenon of the surface dilution is then observed. Otherwise, it appears that the effect of the second element is much more detrimental on the specific activity (TOF) when added to the large particles of RuEC3 in comparison with small particles of RuEC1. It turns out that the four catalysts, RuEC1, RuEC3, RuEC1Snl and RuEC1Ge3, are archetypical of the different behaviours observed in TeMB hydrogenolysis: effects of the size of the Ru particles (RuEC1 and RuEC3), of site segregation (RuEC1Sn1) and of the dilution of Ru surface (RuEC1Ge3). Therefore, the kinetics of TeMB hydrogenolysis was studied in more detail with these catalysts.

Tables 3 and 4 present the results obtained for the RuEC1 sample. It can be seen that as the hydrogen partial pressure is increased, deep hydrogenolysis decreases, reflected by the decrease of the fragmentation factor, the selectivity to TriMB increases, while the selectivity to iC_4 decreases. The change in the product selectivities shows that the central cleavage is becoming less important and the demethylation more so with increasing hydrogen pressure. This is also reflected in the relative rates between the $\alpha\gamma$ and the $\alpha\delta$ processes (Table 4). Fig. 3 shows that, under the experimental conditions investigated, the temperature

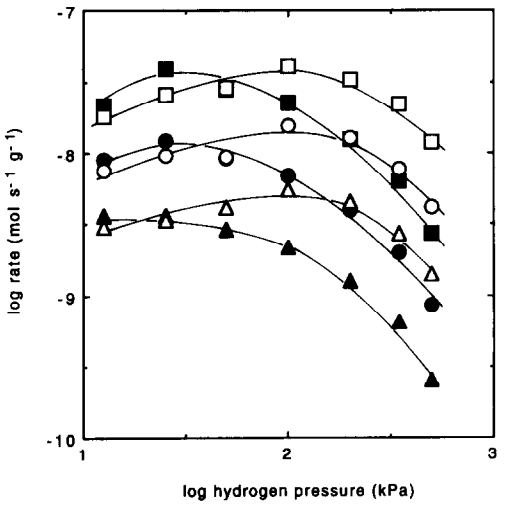

Fig. 3. Hydrogen pressure dependence for the rate of $\alpha\gamma$ (open symbols) and $\alpha\delta$ (full symbols) processes in TeMB hydrogenolysis at different temperatures on RuEC1 catalysts; (□,■) T_R = 476 K, (○,●) T_R = 463 K, (△,▲) T_R = 450 K.

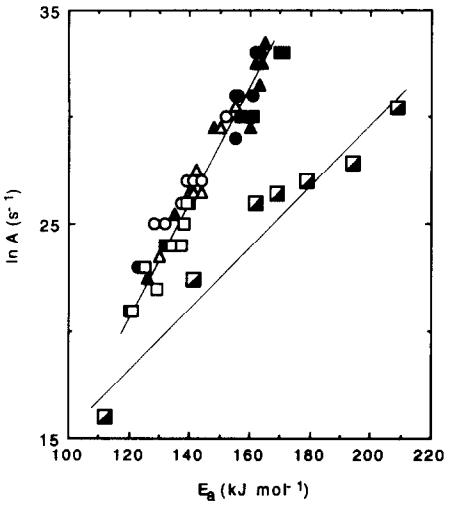

Fig. 4. Compensation effect between E_a and ln$A$ for $\alpha\gamma$ (open symbols) and $\alpha\delta$ (full symbols) processes in TeMB hydrogenolysis at different hydrogen partial pressures over: (○,●) RuEC1, (△,▲) RuEC1Sn1, (□,■) RuEC1Ge3, (◪) RuEC3.

does not have a great effect on the position of the rate maxima for $\alpha\gamma$ and $\alpha\delta$ processes with respect to hydrogen pressure.

The values for the apparent activation energy E_a and the pre-exponential factor A for the $\alpha\gamma$ and $\alpha\delta$ processes were determined by using the simplest expression for the rate law:

$$rate = Ae^{-E_a/RT} \quad (1)$$

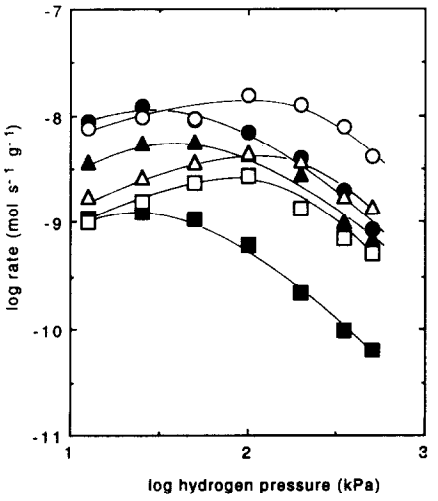

Fig. 5. Hydrogen pressure dependence for the rate of $\alpha\gamma$ (open symbols) and $\alpha\delta$ (full symbols) processes in TeMB hydrogenolysis at 463 K. (○,●) RuEC1, (△,▲) RuEC1Sn1, (□,■) RuEC1Ge3.

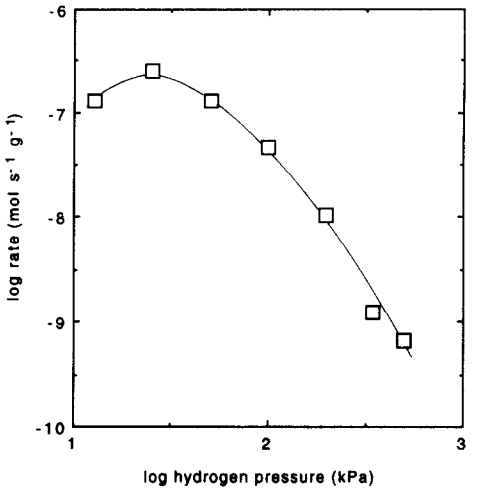

Fig. 6. Hydrogen pressure dependence for the rate of $\alpha\delta$ process in TeMB hydrogenolysis at 463 K over RuEC3.

These values are reported in Table 4 for RuEC1, A being expressed as TOF in s^{-1}. Both terms, A and E_a increase with hydrogen pressure; this observation conforms with the finding of Bond [17] for the hydrogenolysis of propane over a 0.3%Pt/Al_2O_3 catalyst at different reactant pressures.

This behaviour shown by RuEC1 is typical and is observed for all the different catalysts studied. Fig. 4 shows a graph of lnA as a function of E_a for $\alpha\gamma$ and $\alpha\delta$ processes on all the catalysts. It seems that a compensation effect, as described by Bond [17], applies for both the RuEC1 series of catalysts and for RuEC3 respectively. Bond proposed that changing the temperature alters the shape of the kinetic curves by acting on the equilibrium constants for reactant chemisorption and dehydrogenation, i.e. we are measuring apparent activation energies with concentrations of the adsorbed intermediates which change in different ranges as the reactant concentration is changed. There is thus an infinity of values of apparent activation energy that can be measured, depending on the reactant concentration used. One may extend this argument to the case of a series of catalysts, for instance the RuEC1 and RuEC3 series.

The dependence of reaction rate on hydrogen pressure for the RuEC1 series of catalysts and the RuEC3 catalyst is reported in Figs. 5 and 6 respec-

tively. We can see that the ratio between the values of rate maxima for the $\alpha\gamma$ and $\alpha\delta$ processes moves in opposite directions when adding Sn or Ge to the RuEC1 sample.

4. Discussion

The kinetics of TeMB hydrogenolysis in the steady state will be discussed first, with a view to defining better the active sites and the surface complexes involved. For the hydrogenolysis of ethane over a Ru/Al_2O_3 catalyst, Shang and Kenney [18] have proposed several different kinetic models. Bond and Slaa [11] reported recently that the model Shang and Kenney called ES5B, best fits the results for butane hydrogenolysis over the same series of alumina-supported Ru catalysts studied in the present work. This model assumes (i) multisite competitive adsorption between hydrogen and TeMB, (ii) hydrogenation of the dehydrogenated adsorbed alkane (most abundant surface intermediate, MASI) by a surface hydrogen atom as the rate determining step. Using this model, the following reaction steps were assumed for TeMB hydrogenolysis:

$$H_2(g) + 2^* \overset{K_H}{\rightleftharpoons} 2H^* \quad (2)$$

$$C_8H_{18}(g) + (x+1)^* \overset{K_{A(\alpha\gamma)}}{\rightleftharpoons} C_8H^*_{(18-x)} + xH^* \quad (3)$$

$$C_8H^*_{(18-x)} + H^* \overset{k_{\alpha\gamma}}{\rightarrow} C_7H^*_z + CH^*_w \quad (4)$$

for the $\alpha\gamma$ process; and

$$C_8H_{18}(g) + (y+1)^* \overset{K_{A(\alpha\delta)}}{\rightleftharpoons} C_8H^*_{(18-y)} + yH^* \quad (5)$$

$$C_8H^*_{(18-y)} \overset{k_{\alpha\delta}}{\rightarrow} 2C_4H^*_{(18-y+1)/2} \quad (6)$$

for the $\alpha\delta$ process. Where the parameters are defined as follows:

$k_{\alpha\gamma}(k_{\alpha\delta})$ = rate constant for $\alpha\gamma(\alpha\delta)$ process

K_H = adsorption constant of hydrogen

$K_{A(\alpha\gamma)}(K_{A(\alpha\delta)})$ = adsorption constant of TeMB via $\alpha\gamma(\alpha\delta)$ complex

$x(y)$ = the number of hydrogen atoms abstracted from TeMB before bond-breaking for $\alpha\gamma(\alpha\delta)$ process occurs.

Further steps, such as desorption or multiple C-C bond rupture of alkyl fragments, are not rate determining (at low conversion).

Thus, the rates for both the $\alpha\gamma$ and $\alpha\delta$ processes are given by (see Appendix):

$$r_{\alpha\gamma} = \frac{k_{\alpha\gamma}K_AP_A(K_HP_H)^{(x+2y+1)/2}}{\{K_AP_A[(K_HP_H)^{(x/2)} + (K_HP_H)^{(y/2)}] + (K_HP_H)^{(x+y)/2} + (K_HP_H)^{(x+y+1)/2}\}^2} \quad (7)$$

$$r_{\alpha\delta} = \frac{k_{\alpha\delta}K_AP_A(K_HP_H)^{(y+2x+1)/2}}{\{K_AP_A[(K_HP_H)^{(x/2)} + (K_HP_H)^{(y/2)}] + (K_HP_H)^{(x+y)/2} + (K_HP_H)^{(x+y+1)/2}\}^2} \quad (8)$$

Thereafter, an interesting expression for the selectivity can be given:

$$\frac{r_{\alpha\gamma}}{r_{\alpha\delta}} = \frac{k_{\alpha\gamma}K_AP_A(K_HP_H)^{(x+2y+1)/2}}{k_{\alpha\delta}K_AP_A(K_HP_H)^{(y+2x+1)/2}} = \frac{k_{\alpha\gamma}}{k_{\alpha\delta}}(K_HP_H)^{(y-x)/2} \quad (9)$$

Fig. 7 shows the variation of $\log(r_{\alpha\gamma}/r_{\alpha\delta})$ as a function of $\log P_H$ for the RuEC1 catalyst. The linear dependence between these two terms is not excellent but from the value of the slope (≈ 0.5), it seems that one more H atom is abstracted from the $\alpha\delta$ surface complex than from the $\alpha\gamma$ complex before bond-breaking occurs. Moreover, taking into account the hydrogen dependence of the rates in the high pressure region on the RuEC1 based catalysts (Fig. 5), it appears that two or three H atoms at least were removed from TeMB before bond-breaking, but 5 on RuEC3 (Fig. 6). The

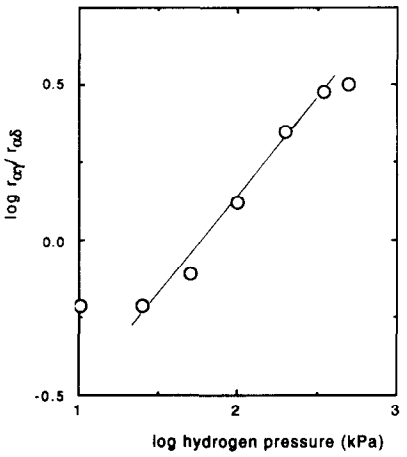

Fig. 7. Hydrogen pressure dependence for the relative rate between $\alpha\gamma$ and $\alpha\delta$ processes in TeMB hydrogenolysis at 483 K over RuEC1.

higher dehydrogenation degree of the $\alpha\delta$ complex on large Ru particles is reflected by the strong inhibiting effect of hydrogen pressure on the reaction rate. On the basis of logical mechanisms and our previous studies on alkane hydrogenolysis on Ru catalysts [3], the following surface complex for TeMB hydrogenolysis can be postulated: Scheme 1 for small Ru particles (RuEC1 catalysts), and Scheme 2 for large Ru particles (RuEC3 catalysts).

The occurrence of both metallacyclobutane and metallacyclopentane during TeMB hydrogenolysis was proved in the case of Rh/Al_2O_3 by deuterium exchange experiments [4]. Moreover, a multisite TeMB adsorption for the $\alpha\delta$ complex (dicarbene or dicarbyne species) on large Ru particles (Eq. 12, Scheme 2) agrees with the difference in sensitivity of $r_{\alpha\delta}$ to hydrogen pressure, or

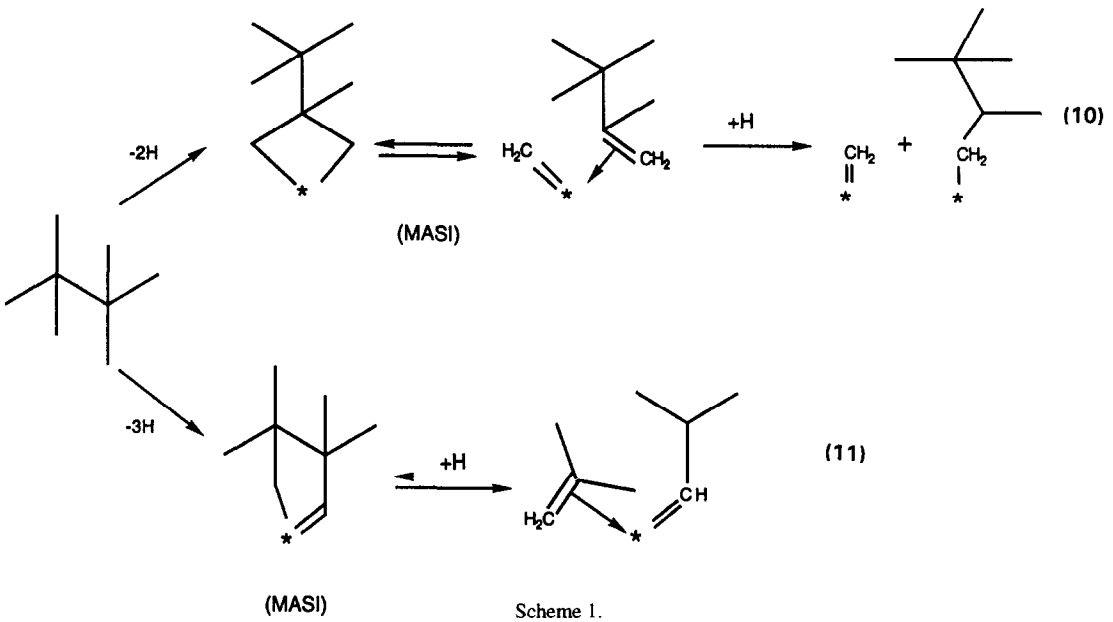

Scheme 1.

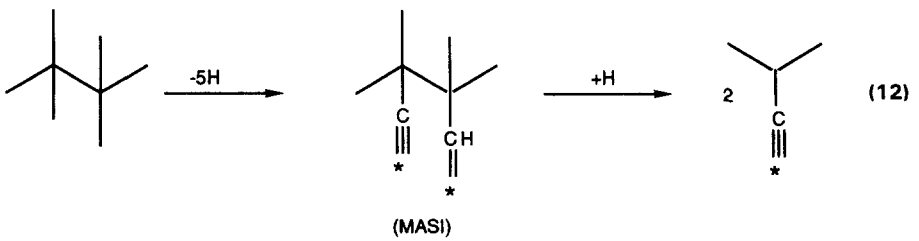

Scheme 2.

Ge addition, on RuEC3 and on the RuEC1 series of catalysts. On small Ru particles, Ge (or Sn) addition has a very small influence on TOF (Table 1), whereas Ge or Sn addition on RuEC3 strongly decreases the activity per Ru site. It is very likely that the $\alpha\delta$ complex needs an 'ensemble' of Ru atoms larger on RuEC3 in comparison with RuEC1 catalysts.

Another important feature with Ru is the occurrence of several consecutive C-C bond ruptures of alkyl fragments before desorption. The extent of which decreases with the metallic dispersion [3]. This behaviour is characterized by the fragmentation factor ξ. Gault [19] suggested that deep fragmentation is favoured on metals showing a capacity to form multiply-bonded species (metallocarbene or metallocarbyne). The TeMB/D_2 exchange results demonstrate that Ru has a strong tendency at higher temperature to form carbene-like intermediates with multiple bonding of a C atom to the surface [5]. These results agree with suggestions that metals with a high activity for hydrogenolysis tend to form metal-carbon multiple bonds [20,21]. The primary fragments, isobutyl or trimethybutyl, formed by a single C-C bond breaking, can suffer either desorption or secondary fragmentation to adsorbed propyl or dimethylbutyl fragments, for instance. In the framework of the 'rake scheme' proposed by Kempling and Anderson [22], Bond and Slaa [23] proposed that the ratio between desorption and further cracking of fragments is given by:

desorption of isobutyl fragment:

$$r_d = k' \theta_{iC_4} P_H^a \quad (13)$$

cracking of the isobutyl fragment:

$$r_c = k^* \theta_{iC_4} P_H^b \quad (14)$$

$(a\text{-}b)$ = difference in number of H_2 molecules needed for desorption and further cracking respectively.

The value of $(a-b)$ is given by the slope of the graph of $\log(S_{iC4}/(S_{\alpha\delta}-S_{iC4}))$ plotted as a function of $\log P_H$; $S_{\alpha\delta}$ and S_{iC4} being the selectivities for the overall $\alpha\delta$ process ($iC_4+C_3+C_2$) and for isobutane respectively. The same approach can be applied to the trimethybutyl fragment. Fig. 8 shows such a plots for RuEC1 and RuEC3 catalysts. The desorption of isobutyl fragments from large Ru particles needs one more H_2 molecule than desorption from small Ru particles. This point emphasizes the much higher dehydrogenation degree of that fragment on RuEC3 (Eq. 12, Scheme 2). However, from Fig. 8a it is note-

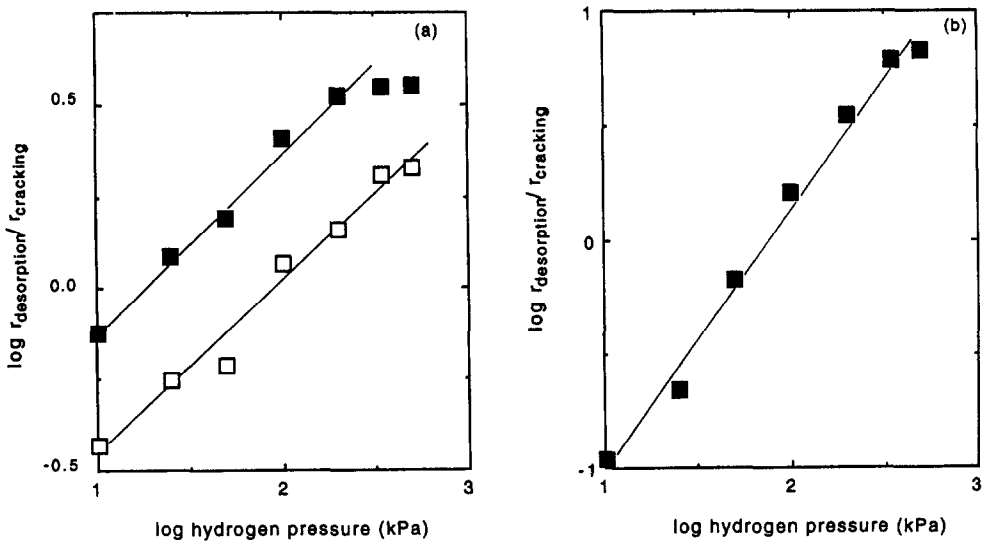

Fig. 8. Hydrogen pressure dependence for the relative rate between desorption and cracking of the adsorbed alkyl fragments: (■) isobutyl, (□) trimethylbutyl. (a) RuEC1 at 483 K, (b) RuEC3 at 433 K.

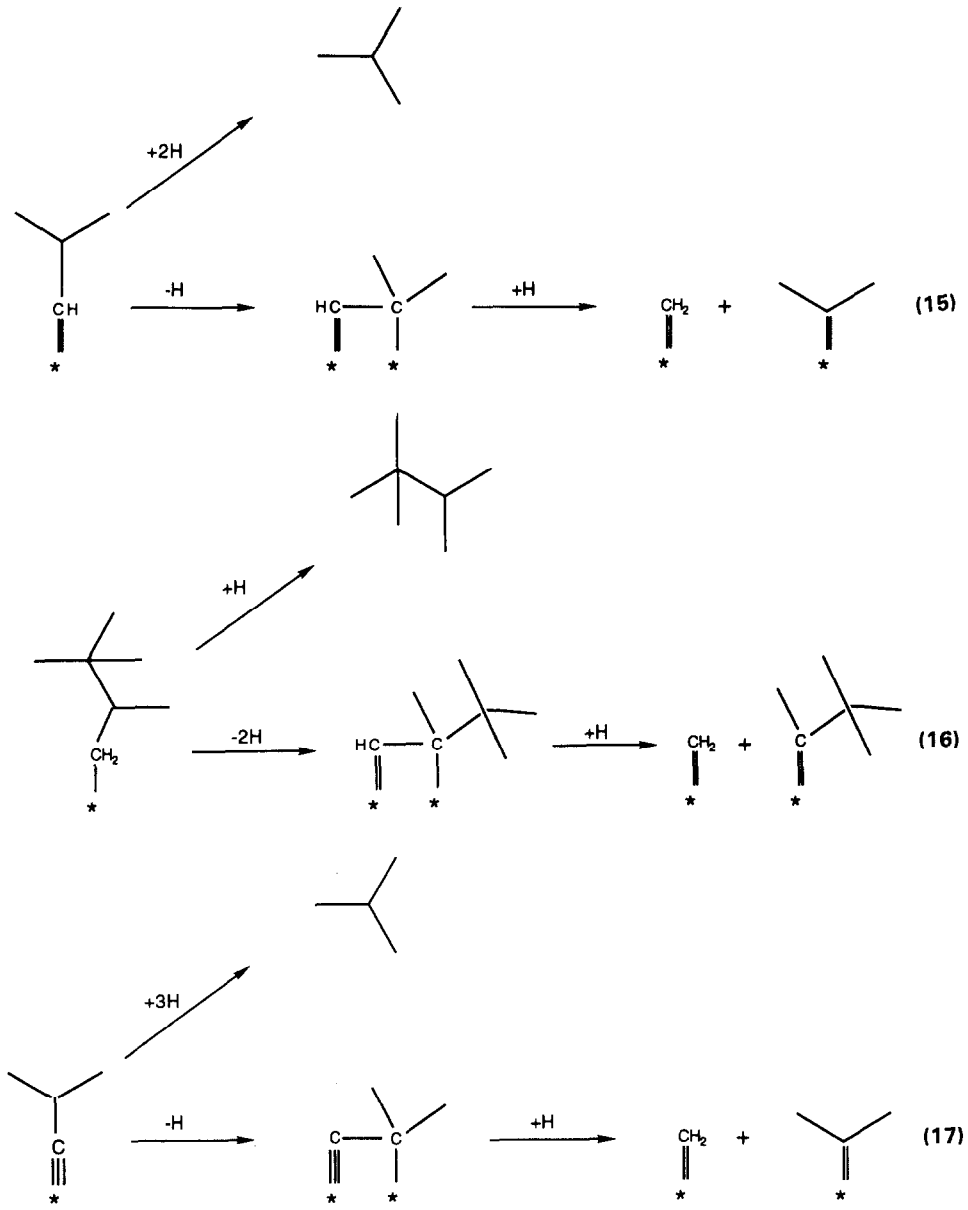

Scheme 3.

worthy that trimethybutyl and isobutyl fragments need the same difference in the number of H atoms to be desorbed or cracked in the adsorbed state on the RuEC1 sample. A possible sequence of further cracking of isobutyl and trimethybutyl fragments on both small (Eqs. 15, 16) and large (Eq. 17) Ru particles is shown in Scheme 3.

It emerges from this study that the mechanism of TeMB hydrogenolysis shows differences depending on the size of Ru particles. On small aggregates, both $\alpha\gamma$ and $\alpha\delta$ routes proceed through metallacycles bonded onto a small ensemble of Ru atoms (one Ru atom?). The two surface entities, metallacyclobutane ($\alpha\gamma$) and metallacyclopentane ($\alpha\delta$), are little dehydrogenated, only 2 or 3 H atoms are abstracted. The rate determining step is C-C bond-breaking in the metallacycle by attack with an H atom. In both cases, a

carbene/π-alkene adsorbed species is formed. The alkene species can rearrange to form a metallocarbene through α-β hydrogen shift [19]. The similarity between both mechanisms for the $\alpha\gamma$ and $\alpha\delta$ routes would be further supported by the compensation effect between E_a and lnA observed for $\alpha\gamma$ and $\alpha\delta$ reaction rates at different H_2 pressures on RuEC1, RuEC1Sn1 and RuEC1Ge3 (Fig. 4).

On large aggregates, the $\alpha\delta$ route is the prevailing process (>90%) occurring through 1-4 multibonded species on a large ensemble of Ru atoms. This surface species is highly dehydrogenated with the abstraction of 5 H atoms at least. After bond-breaking between the two C_Q atoms has occurred, adsorbed carbyne species remain at the surface. A compensation effect also exists between E_a and lnA for the reaction rate at different H_2 pressures (Fig. 4). The fact that this compensation effect does not coincide with that derived on the RuEC1 series of catalysts could be an argument emphasizing the difference of mechanism and/or reactive sites for TeMB hydrogenolysis on large and small Ru particles.

From these sudies, it seems that on large Ru particles the prevailing reaction is the $\alpha\delta$ process occuring on an ensemble site containing several Ru atoms. This specificity makes the reaction rate sensitive to dilution of the Ru surface into smaller ensembles when adding Sn or Ge. Indeed, the TOF is divided by 20 in that case.

As mentioned briefly above, on small Ru aggregates the reactive sites for both $\alpha\gamma$ and $\alpha\delta$ routes are formed by small ensembles of few Ru atoms. Therefore, the specific reaction rate is less sensitive to the bimetallic effect. Indeed, at the maximum of the rate as a function of H_2 pressure, the $TOF_{\alpha\delta}$ remains unchanged after Sn addition (RuEC1Sn1), and decreased by 5 upon Ge addition (RuEC1Ge3). On the other hand, the $TOF_{\alpha\gamma}$ is divided by 1.7 upon Sn addition and by 2.3 upon Ge addition. Since the mechanisms for both the $\alpha\gamma$ and $\alpha\delta$ routes were basically not changed upon addition of a second element to RuEC1, the difference in the values of the maxima in the rate dependence of the catalyst reflects changes in the rate constant $k_{\alpha\gamma}$ and $k_{\alpha\delta}$ which can be expressed as:

$$k_{\alpha\gamma}=k^0_{\alpha\gamma}e^{-\frac{E}{RT}} \text{ and } k_{\alpha\delta}=k^0_{\alpha\delta}e^{-\frac{E}{RT}} \qquad (18)$$

where $E_t(E'_t)$ is the true activation energy, and $k^0_{\alpha\gamma}(k^0_{\alpha\delta})$ the pre-exponential factor which contains the entropy term and the number of active sites. There is no change in the number of active sites for the $\alpha\delta$ process upon Sn addition. It was concluded for Pt [2], Rh [1] and Ru [3] catalysts that the $\alpha\delta$ process occurs on the sites of highest coordination of a given particle. Thereafter, the preferential location of Sn at defect sites, corners and edges, in RuSn aggregates is confirmed in a situation not obscured by kinetic artefacts due to differences in H_2 pressure dependence of $\alpha\gamma$ and $\alpha\delta$ routes. The same approach, developed for RuGe aggregates, shows that Ge does not have such a definite site preference. This behaviour seems to be confirmed by EXAFS experiments [16] and quantum chemical calculations on bimetallic model clusters [24,25]. EXAFS of RuEC1, RuEC1Sn1 and RuEC1Ge3 shows that Ge is more diluted in the Ru matrix than Sn [16]. From quantum chemical calculations on Ru_9, Ru_8Ge and Ru_8Sn clusters by means of the functional density method, we concluded that Sn, and Ge to a much smaller extent, prefer to be localized at the sites of lower coordination [24]. Similar calculations on Ru_{13}, $Ru_{10}Ge_3$ and $Ru_{10}Sn_3$ clusters with perfect cubooctahedral shape emphasized that Ge-Ge bonds are less favoured than Sn-Sn bonds at the surface of these aggregates, all surface atoms having the same coordination number of 5 [25].

All the kinetic experiments were carried out at the steady state on a carbon pre-covered Ru surface. Hence, it is tempting to speculate on how this 'carbon deposit' is distributed over the surface. By comparing the effects on the selectivity of the deposited carbon (Fig. 1b) and Sn and Ge addition (Table 2 and Fig. 4), more similarities appear between the effects of Ge and carbon than with Sn. We can then postulate that the carbon deposit is laid down on the Ru surface in a rather random fashion.

5. Conclusions

Our previous works based on the comparison of selectivities in the C-C cleavage in model alkanes, on Ru catalysts of widely varying dispersions and on Ru 'alloys', supported the conclusion of a preferential location of Sn and Pb at sites of low coordination, corner and edge sites, and a location of Ge in a more random fashion. The present study of the kinetics of TeMB hydrogenolysis on model mono- and bimetallic Ru catalysts confirms this hypothesis, in a wide range of H_2 pressure.

TeMB hydrogenolysis occurs through two main routes, central cleavage between the two quaternary carbon atoms leading to isobutane ($\alpha\delta$ process), demethylation to 2,2,3-trimethylbutane ($\alpha\gamma$ process). The kinetic results can be rationalized assuming that different kinds of surface intermediates are involved in this reaction, the nature of which is depending on both the size of Ru particles and the process considered. Large Ru particles favour the formation of highly dehydrogenated species, metallocarbenes and metallocarbynes, bonded to several Ru atoms ('large ensembles'). On small Ru particles, less dehydrogenated metallacycles bonded to a small number of Ru atoms ('small ensemble') are prevailing. The $\alpha\gamma$ process is going through metallacyclobutane and the $\alpha\delta$ process through metallacyclopentane, the former being less dehydrogenated than the latter.

Acknowledgements

This works forms part of the EC-funded 'Stimulation Action' programme SC1*-CT91-0681. E. Crabb thanks the EEC for granting her research. The authors thank Prof. G.C. Bond for fruitful comments.

Appendix 1

The application of the Langmuir equation for the adsorption of H_2 and TeMB gives:

$$K_H P_H \theta_v^2 = \theta_H^2, \text{ and } \theta_v = \theta_H / (K_H P_H)^{1/2} \quad (19)$$

$$K_{A(\alpha\gamma)} P_A \theta_v^{x+1} = \theta_H^x \theta_{\alpha\gamma} \quad (20)$$

$$K_{A(\alpha\delta)} P_A \theta_v^{y+1} = \theta_H^y \theta_{\alpha\delta} \quad (21)$$

θ_H, $\theta_{\alpha\gamma}$, $\theta_{\alpha\delta}$ and θ_v are the surface coverages of H, $C_8H_{(18-x)}$, $C_8H_{(18-y)}$ and vacant sites respectively. For competitive adsorption between H_2 and TeMB,

$$\theta_H + \theta_{\alpha\gamma} + \theta_{\alpha\delta} + \theta_v = 1 \quad (22)$$

Incorporating Eq. 19, the expressions for $\theta_{\alpha\gamma}$ and $\theta_{\alpha\delta}$ reduce to

$$\theta_{\alpha\gamma} = \theta_v K_{A(\alpha\gamma)} P_A / (K_H P_H)^{x/2} \quad (23)$$

$$\theta_{\alpha\delta} = \theta_v K_{A(\alpha\delta)} P_A / (K_H P_H)^{y/2} \quad (24)$$

Assuming that $K_{A(\alpha\gamma)} = K_{A(\alpha\delta)} = K_A$, and solving Eqs. 22 to 24, give the expressions for θ_H, $\theta_{\alpha\gamma}$ and $\theta_{\alpha\delta}$ as

$$\theta_H = \frac{(K_H P_H)^{(x+y+1)/2}}{K_A P_A [(K_H P_H)^{(x/2)} + (K_H P_H)^{(y/2)}] + (K_H P_H)^{(x+y)/2} + (K_H P_H)^{(x+y+1)/2}} \quad (25)$$

$$\theta_{\alpha\gamma} = \frac{(K_A P_A)(K_H P_H)^{y/2}}{K_A P_A [(K_H P_H)^{(x/2)} + (K_H P_H)^{(y/2)}] + (K_H P_H)^{(x+y)/2} + (K_H P_H)^{(x+y+1)/2}} \quad (26)$$

$$\theta_{\alpha\delta} = \frac{(K_A P_A)(K_H P_H)^{x/2}}{K_A P_A [(K_H P_H)^{(x/2)} + (K_H P_H)^{(y/2)}] + (K_H P_H)^{(x+y)/2} + (K_H P_H)^{(x+y+1)/2}} \quad (27)$$

The rate determining steps for $\alpha\gamma$ and $\alpha\delta$ processes are described by Eqs. 4 and 6, respectively. Thus, the rate equation for the $\alpha\gamma$ process is given by

$$r_{\alpha\gamma} = k_{\alpha\gamma} \theta_{\alpha\gamma} \theta_H = \frac{k_{\alpha\gamma} K_A P_A (K_H P_H)^{(x+2y+1)/2}}{\{K_A P_A [(K_H P_H)^{(x/2)} + (K_H P_H)^{(y/2)}] + (K_H P_H)^{(x+y)/2} + (K_H P_H)^{(x+y+1)/2}\}^2} \quad (28)$$

Similarly for the $\alpha\delta$ process

$$r_{\alpha\delta} = k_{\alpha\delta}\theta_{\alpha\gamma}\theta_H =$$

$$\frac{k_{\alpha\delta}K_A P_A (K_H P_H)^{(x+2y+1)/2}}{\{K_A P_A[(K_H P_H)^{(x/2)} + (K_H P_H)^{(y/2)}] + (K_H P_H)^{(x+y)/2} + (K_H P_H)^{(x+y+1)/2}\}^2} \quad (29)$$

References

[1] B. Coq, A. Goursot, T. Tazi, F. Figuéras and D. Salahub, J. Am. Chem. Soc., 113 (1991) 1485.

[2] B. Coq, A. Chaqroune, F. Figuéras and B. Nciri, Appl. Catal. A, 82 (1992) 231.

[3] B. Coq, A. Bittar and F. Figuéras, Appl. Catal., 59 (1990) 103.

[4] R. Brown, C. Kemball and I.H. Sadler, in Proceedings 9th International Congress on Catalysis, Calgary, 1988, Chemical Institute of Canada, Ottawa, 1988, Vol.3, p. 1013.

[5] R. Brown and C. Kemball, J. Chem. Soc., Faraday Trans., 89 (1993) 585.

[6] C. Kemball, personal communication.

[7] B. Coq, A. Bittar, R. Dutartre and F. Figuéras, J. Catal., 128 (1991) 275.

[8] J.J. Burton, E. Hyman and D.G. Fedak, J. Catal., 37 (1975) 106.

[9] B. Coq, R. Dutartre, F. Figuéras and A. Rouco, J. Phys. Chem., 93 (1989) 4904.

[10] M.W. Smale and T.S. King, J. Catal., 125 (1990) 335.

[11] G.C. Bond and J.C. Slaa, J. Mol. Catal., 89 (1994) 221.

[12] B. Coq, E. Crabb, M. Warawdekar, G.C. Bond, J.C. Slaa, S. Galvagno, L. Mercadante, J. Garcia Ruiz, M.C. Sanchez Sierra, J. Mol. Catal., 92 (1994) 107.

[13] C. Travers, T.D. Chan, R. Snappes and J.P. Bournonville, US Pat. 4,456,775, 1984

[14] J. Margitfalvi, M. Hegedus, S. Gobolos, E. Kern Talas, P. Szedlacsek, S. Szabo and F. Nagy, in Proceedings 8th International Congress on Catalysis, Berlin, 1984, Verlag Chemie, Weinheim, 1984, Vol.4, p.903.

[15] Z. Paál and P. Tétényi, Nature (London), 267 (1977) 234

[16] J. Garcia Ruiz and M.C. Sanchez Sierra, J. Mol. Catal., accepted.

[17] G.C. Bond, Catal. Today, 17 (1993) 399.

[18] S.B. Shang and C.N. Kenney, J. Catal., 134 (1992) 134.

[19] F.G. Gault, in Advances in Catalysis, Academic Press, London and New York, 1981, Vol. 30, p. 1.

[20] C. Kemball, Catal. Rev., 5 (1971) 33.

[21] E.H. van Broekhoven and V. Ponec, J. Mol. Catal., 25 (1984) 109.

[22] J.C. Kempling and R.B. Anderson, Ind. Eng. Chem. Process Res. Dev., 11 (1972) 146.

[23] G.C. Bond and J.C. Slaa, J. Mol. Catal., submitted.

[24] A. Goursot, L. Pedocchi and B. Coq, J. Phys. Chem., 98 (1994) 8747.

[25] A. Goursot, L. Pedocchi and B. Coq, J. Phys. Chem., in preparation.